PHYSICAL REVIEW B **90**, 100402(R) (2014)

Magnetic ordering of hyperfine-coupled nuclear and 4*f*-electron moments in the clathrate compound $Pr_3Pd_{20}Ge_6$

O. Iwakami,[1,*] Y. Namisashi,[1] S. Abe,[1] K. Matsumoto,[1] G. Ano,[2] M. Akatsu,[3] K. Mitsumoto,[2] Y. Nemoto,[2] N. Takeda,[4] T. Goto,[2] and H. Kitazawa[5]

[1]*Department of Physics, Kanazawa University, Kanazawa 920-1192, Japan*
[2]*Graduate School of Science and Technology, Niigata University, Niigata 950-2181, Japan*
[3]*Department of Physics, Niigata University, Niigata 950-2181, Japan*
[4]*Faculty of Engineering, Niigata University, Niigata 950-2181, Japan*
[5]*National Institute for Materials Science, Tsukuba 305-0047, Japan*

(Received 6 March 2014; revised manuscript received 6 August 2014; published 4 September 2014)

Complex ac susceptibility, $\chi = \chi' - i\chi''$, measurements of the clathrate compound $Pr_3Pd_{20}Ge_6$ were performed in static fields up to 10 mT for $H \parallel [001]$ and at temperatures down to 500 μK. Praseodymium (Pr) nuclear magnetic moments at the 8*c* site, where quadrupole moments of 4*f* electrons order at $T_{Q1} = 250$ mK, were found to order antiferromagnetically at 9 mK, as shown by a peak in χ' and a substantial increase in thermal relaxation time. The large enhancement factor $(1 + K_{8c})$ obtained by calculation of the hyperfine-enhanced nuclear susceptibility of Pr at the 8*c* site accounts for the high transition temperature of Pr nuclear magnetic moments and the large χ' below 30 mK. From analysis of the crystalline electric field and the mean-field approximation, we conclude that a χ peak at 77 mK can be ascribed to an antiferromagnetic ordering of magnetic moments of 4*f* electrons at the 4*a* site. We found that nuclear and *f*-electron moments order separately on two sublattices in this compound. The temperature and magnetic field dependence of χ' and χ'' between 30 and 60 mK are discussed in terms of dissipation phenomena.

DOI: 10.1103/PhysRevB.90.100402 PACS number(s): 75.30.Kz, 71.70.Jp, 82.75.−z, 31.30.Gs

The nuclear magnetic moment is about two thousandths of the electron magnetic moment, so the interaction among nuclear spins is roughly six orders of magnitude weaker than that among electron spins. This means that usually nuclear magnetic ordering temperatures are on the order of a microkelvin or a much lower temperature region, where demagnetization of nuclear spins themselves is required. In Van Vleck paramagnets, nuclear spins strongly couple with *f*-electron spins through the hyperfine (HF) interaction, and nuclear magnetic ordering occurs at millikelvin or submillikelvin temperatures, because nuclear moments are enhanced by a factor of over ten by HF coupling. This hyperfine-enhanced (HFE) nuclear magnetism has been studied in intermetallic compounds of praseodymium (Pr). The HFE nuclear magnetic ordering has been observed in several materials with a singlet crystalline electric field (CEF) ground state, such as $PrNi_5$, $PrIn_3$, and $PrCu_6$ [1–4].

In cubic Pr compounds, the ninefold degenerate $\boldsymbol{J} = 4$ multiplet of Pr^{3+} ions is split into a Γ_1 singlet, non-Kramers Γ_3 doublet, Γ_4, and Γ_5 triplets by CEF effects. The Γ_3 doublet possesses no magnetic dipole degree of freedom but does have electric quadrupole and magnetic octupole degrees of freedom. The Γ_3 ground state system has attracted much interest with respect to quadrupole ordering and the quadrupole Kondo effect [5–8]. There is also a possibility of HFE nuclear magnetic ordering, since the Γ_3 doublet exhibits Van Vleck paramagnetism at low temperatures. The interplay with electrons must bring the diversity in HFE nuclear magnetism, so it is intriguing to study the Pr nuclear spin in the phase where the 4*f* electrons exhibit electric quadrupole ordering. However, HFE nuclear ordering in the electric quadrupole ordered phase has been observed only in $PrPb_3$ at 5 mK [9]. In $PrPb_3$, the exotic antiferromagnetic (AFM) structures due to the two different antiferroquadrupole (AFQ) sublattices have been predicted [4].

Recently, there has been growing interest in Pr compounds with cage structures. $PrTi_2Al_{20}$ has a non-Kramers Γ_3 ground state and shows a superconducting transition in the phase where 4*f* electrons are ferroquadrupole (FQ) ordered [10]. In this material, HFE Pr nuclear ordering has been predicted from a muon spin rotation (μSR) study [11]. In the filled skutterudite $PrRu_4P_{12}$ and the clathrate compound $Pr_3Pd_{20}Si_6$, the formation of new multiplets caused by the HF interaction between nuclear and *f*-electron spins has been studied theoretically and experimentally [12,13]. Anomalous transport properties observed below 10 K in $PrRu_4P_{12}$ [14] and a new phase transition at 60 mK in $Pr_3Pd_{20}Si_6$ [13] have been reported, but these properties are still unsolved. Novel physical properties due to the HF interaction are expected in these Pr-based compounds, so it is interesting to study Pr nuclear ordering and the correlation among nuclear, *f*-electron, and conduction electron spins.

$R_3Pd_{20}X_6$ (R = rare earth and uranium, X = Ge, Si) have a cubic $Cr_{23}C_6$-type structure with a space group $Fm\bar{3}m$. The R atoms occupy two crystallographically inequivalent sites: 4*a* sites with O_h symmetry, and 8*c* sites with T_d symmetry. $R_3Pd_{20}X_6$ have attracted much attention because of their characteristic magnetic ordering with two different propagation vectors on two sublattices, and the quadrupole ordering of *f* electrons [15–19]. In particular, $R_3Pd_{20}Ge_6$ have been studied intensively from the viewpoint of rattling motions of a guest rare-earth ion in an oversized cage that are not observed in $R_3Pd_{20}Si_6$ [20,21].

The Pr-based compound $Pr_3Pd_{20}Ge_6$ shows quadrupole order of 4*f* electrons and rattling motions of Pr atoms at the 4*a* site [22]. The CEF level schemes of Pr^{3+} ions at the

*Corresponding author: ou4.e-66@stu.kanazawa-u.ac.jp

4*a* and 8*c* sites, as determined by inelastic neutron scattering and magnetization experiments, are Γ_5(0 K)-Γ_3(5.4 K)-Γ_4(50 K)-Γ_1(113 K) and Γ_3(0 K)-Γ_5(6 K)-Γ_4(46 K)-Γ_1(111 K), respectively [23,24]. The ground state at the 4*a* site is a magnetic Γ_5 triplet that has three magnetic dipoles J_x, J_y, J_z and five quadrupoles O_u, O_v, O_{xy}, O_{yz}, O_{zx}, while that at the 8*c* site is a nonmagnetic Γ_3 doublet that has two quadrupoles O_u, O_v and an octupole T_{xyz}. This material is an excellent candidate to study HF interaction between nuclear and f-electron moments.

According to ultrasound measurements of $Pr_3Pd_{20}Ge_6$ at zero magnetic field [22], the elastic constants $(C_{11} - C_{12})/2$ and C_{44} exhibited considerable softening below 10 K and showed minima at $T_{Q1} = 250$ mK and $T_{Q2} = 60$ mK, respectively. The analysis of elastic constants indicated that the minima at T_{Q1} and T_{Q2} were ascribed to the AFQ ordering of the Γ_3 doublet at the 8*c* site and the FQ ordering of the Γ_5 triplet at the 4*a* site, respectively. However, the dc magnetic susceptibility of $Pr_3Pd_{20}Ge_6$ shows no anomaly down to 80 mK [25]. The magnetic property of the Γ_5 triplet ground state at the 4*a* site with rattling motions is an open question. Furthermore, no nuclear order has been reported in $Pr_3Pd_{20}X_6$. Nontrivial Pr nuclear order due to the HF interaction is expected in the f-electron quadrupole ordered states. Therefore, we have performed ac susceptibility measurements of $Pr_3Pd_{20}Ge_6$ at very low temperatures.

The single crystal used in our investigation was from the same batch of high-quality samples, grown by a floating zone method, for which ultrasound measurements were reported [22]. The sample, about $4 \times 4 \times 6$ mm^3 in size, was cooled with a copper nuclear demagnetization refrigerator and a ^{3}He-^{4}He dilution refrigerator down to 500 μK. The temperature was measured by a Pt-NMR thermometer, a ^{3}He melting curve thermometer, and a RuO_2-resistance thermometer.

The complex ac susceptibility $\chi = \chi' - i\chi''$ was measured by a mutual inductance technique, using the same experimental setup as described in Ref. [26]. The ac excitation field (frequency 16 Hz) and the external static field (up to 10 mT) were parallel to the [001] crystalline axis. The amplitude of the ac field was 1.5 μT above 10 mK, but was reduced to 0.15 μT below 10 mK to suppress eddy-current heating. χ' was normalized to the absolute value using the dc susceptibility measured by a superconducting quantum interference device (SQUID) magnetometer (Quantum Design) between 2 and 4 K.

Figure 1 shows the temperature dependence of χ' of $Pr_3Pd_{20}Ge_6$ in zero static field below 4 K. χ' increases monotonically with decreasing temperature down to about 80 mK. We confirmed that the magnetic susceptibility showed no sign of magnetic ordering at the AFQ ordering temperature, $T_{Q1} =$ 250 mK. These results are consistent with the previous dc susceptibility measurements reported by Amitsuka *et al.* [25]. The lines displayed in Fig. 1 are the calculated results based on the CEF level scheme and the mean-field approximation. In $R_3Pd_{20}X_6$, neutron diffraction experiments demonstrated that the magnetic ordering at the 4*a* and 8*c* sites occurs independently at different temperatures [15–17]. Furthermore, the CEF level schemes of the 4*a* and 8*c* sites in $Pr_3Pd_{20}Ge_6$ are different. Therefore, the magnetic susceptibility of $Pr_3Pd_{20}Ge_6$ could be obtained by the sum of the contributions from both sites. The 4f-electron magnetic susceptibility of each site is

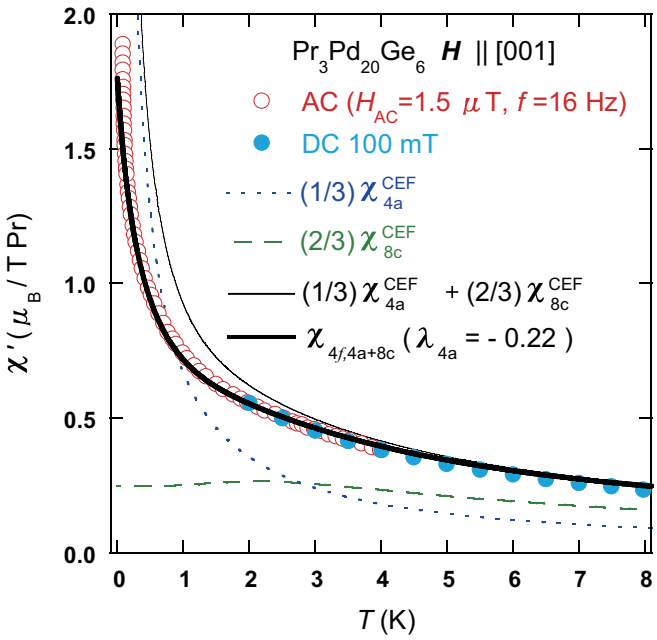

FIG. 1. (Color online) Temperature dependence of the susceptibility of single crystalline $Pr_3Pd_{20}Ge_6$ along the [001] axis. The open circles are the real part of the ac susceptibility in zero static magnetic field. The solid circles are dc susceptibility in a static field of 100 mT. The dotted line and dashed line represent the susceptibilities for 4*a* and 8*c* sites that are calculated from the CEF level schemes with no exchange interaction, respectively. The total susceptibility with no exchange interaction is represented as a solid line. The bold solid line denotes total susceptibility in the case where the Pr atom at the 4*a* site has an antiferromagnetic interaction.

expressed as $1/\chi_{4f,i} = 1/\chi_i^{\rm CEF} - \lambda_i$ $(i = 4a, 8c)$, where $\chi_i^{\rm CEF}$ are the single-ion magnetic susceptibilities calculated from the CEF level scheme, and λ_i are the molecular field coefficients. The total susceptibility $\chi_{4f,4a+8c}$ is expressed (note that the occupation ratio of $4a : 8c = 1 : 2$) as $\chi_{4f,4a+8c} = (1/3)\chi_{4f,4a} + (2/3)\chi_{4f,8c}$. Our experimental results give $\lambda_{4a} = -0.22$ and $\lambda_{8c} = 0$ T/$\mu_{\rm B}$. The negative λ_{4a} indicates an AFM interaction between 4f-dipole moments at the 4*a* site.

Figure 2 shows both components of the susceptibility as functions of temperature between 20 and 120 mK in static fields of 0, 3, 5, and 10 mT. χ' shows a significant field dependence below 90 mK. Both χ' and χ'' have a sharp peak at $T_{N1} = 77$ mK in zero static field. Upon application of magnetic fields, the peak temperature does not change, but the peak height diminishes. The field dependence of the peak temperature and the negative λ_{4a} indicate that the AFM ordering of the Γ_5 triplet at the 4*a* site occurs at T_{N1}. It is possible that this transition corresponds to that observed by ultrasound measurements at T_{Q2} [22]. The difference in transition temperatures of these two measurements may be caused by a sample dependence because the $R_3Pd_{20}X_6$ phase possesses a very narrow homogeneous range [27]. The interplay between 4f electrons at the 4*a* site is an important issue. The complicated temperature variation of susceptibility between 70 and 30 mK will be discussed later.

Figure 3(a) shows χ' as a function of temperature down to 500 μK in static fields of 0, 3, 5, and 10 mT. As mentioned above, the ac excitation field was reduced below 10 mK; this

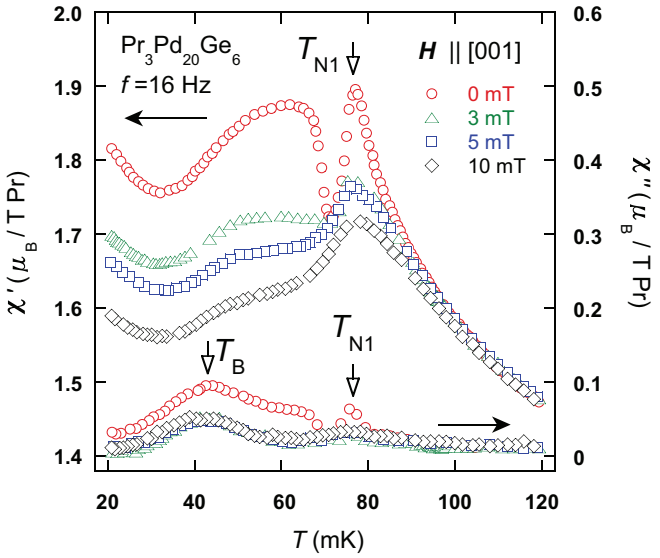

FIG. 2. (Color online) Both components of the ac susceptibility of single crystalline $Pr_3Pd_{20}Ge_6$ as a function of temperature between 20 and 120 mK in static fields of 0, 3, 5, and 10 mT along the [001] axis. The open arrows represent the susceptibility peaks at $T_{N1} = 77$ mK and $T_B = 43$ mK.

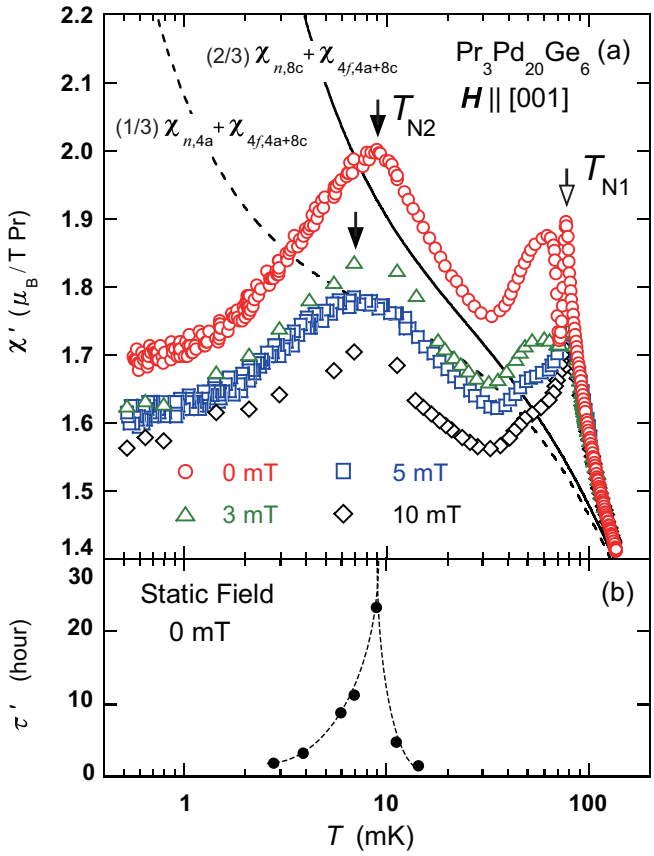

FIG. 3. (Color online) (a) Temperature dependence of the real part of the ac susceptibility in static fields of 0, 3, 5, and 10 mT along the [001] axis. The solid arrows represent the nuclear magnetic transition at T_{N2}. The solid and dashed lines represent $(2/3)\chi_{n,8c} + \chi_{4f,4a+8c}$ and $(1/3)\chi_{n,4a} + \chi_{4f,4a+8c}$, respectively. (b) Thermal relaxation times of the ac susceptibility after a temperature change around 9 mK.

meant that χ' became very scattered, and changes in χ'' were not discernible from the scatter. χ' increases again below 30 mK and shows a peak at $T_{N2} = 9$ mK in zero static field. The susceptibility peak becomes smaller and shifts slightly to lower temperatures with increasing static fields. From the analysis in terms of the HFE Pr nuclear magnetism and measurements of the thermal relaxation time (see below), we concluded that these peaks can be attributed to AFM nuclear ordering at the 8*c* site.

The HFE single-ion nuclear magnetic susceptibility of a Pr nucleus at each site can be expressed by the Curie law as $\chi_{n,i} = g_n^2\mu_n^2 I(I+1)(1+K_i)^2/3k_BT$ $(i = 4a, 8c)$, where g_n, μ_n, and k_B are the nuclear g factor, the nuclear magneton, and the Boltzmann constant, respectively. The enhancement factor $1 + K_i$ is expressed as $K_i = \Lambda_i g_J \mu_B A/(1-\eta_i) g_n \mu_n$, where A is the HF coupling constant $A \simeq +0.052$ K [28,29], the inverse of $1-\eta_i$ $(\eta_i = \lambda_i g_J^2 \mu_B^2 \Lambda_i)$ depends on the exchange interaction between $4f$ electrons, and Λ_i is calculated from the nondiagonal matrix elements of J_z and the energy differences between excited and ground states. The enhancement factors for the Pr nuclei at the 4*a* and 8*c* sites were calculated by using λ_i obtained by CEF analysis and evaluated as $1 + K_{4a} \simeq 23.7$ and $1 + K_{8c} \simeq 39.4$. Those enhancement factors are the averaged values of the enhancement factors for each eigenstate of CEF ground state.

At very low temperatures, the observed susceptibility mainly consists of Pr nuclear and $4f$-electron susceptibilities. The $4f$-electron susceptibility has already been calculated using the CEF level schemes and plotted as the bold solid line, $\chi_{4f,4a+8c}(\lambda_{4a} = -0.22, \lambda_{8c} = 0\,\mathrm{T}/\mu_B)$, in Fig. 1. To elucidate the effect of HFE Pr nuclear spins on the observed susceptibility, we plotted $(2/3)\chi_{n,8c} + \chi_{4f,4a+8c}$ and $(1/3)\chi_{n,4a} + \chi_{4f,4a+8c}$ as shown by the solid and dashed lines in Fig. 3(a), respectively. The solid line almost agrees with the experimental results above T_{N2}. Therefore, the susceptibility increase below 30 mK is accounted for principally by the HFE Pr nuclear magnetism caused by the Γ_3 ground state at the 8*c* site. The HFE nuclear magnetism due to the non-Kramers Γ_3 ground state has been observed in several materials, such as $PrMg_3$, $PrPb_3$, and PrV_2Al_{20} [7,9,30]. On the other hand, the increase in χ' expected from the Pr nuclei at the 4*a* site as shown by the dashed line was not observed down to the lowest temperature. This result suggests that the nuclear spin degrees of freedom at the 4*a* site are suppressed in this temperature range.

We found that the thermal relaxation time of the susceptibility at zero static field becomes considerably longer around $T_{N2} = 9$ mK, reaching 24 h. χ' relaxation after a temperature change could be fitted with a single exponential law $\exp(-t/\tau')$ as a function of time. Figure 3(b) shows the temperature dependence of the thermal relaxation time τ'. In agreement with the susceptibility peak, τ' has a sharp peak at T_{N2}. In this thermal relaxation process, τ' is given as $\tau' = R_B C$, where C represents the sample heat capacity, and R_B is the boundary resistance between the thermal link and the sample. Usually, R_B is inversely proportional to temperature. Therefore, the peak of relaxation time indicates that the heat capacity has a maximum at T_{N2}. The significant increase in τ' in the vicinity of the HFE nuclear magnetic phase transition temperature of

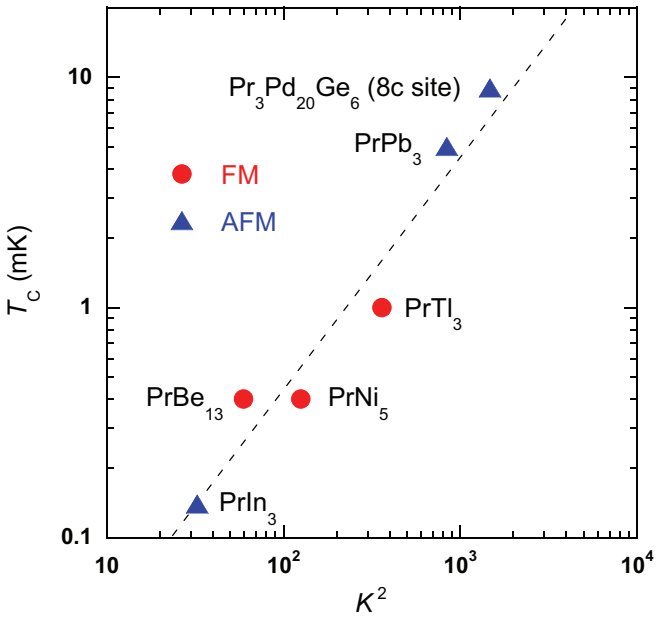

FIG. 4. (Color online) Hyperfine-enhanced Pr nuclear magnetic ordering temperatures as a function of K squared. The circles and triangles indicate ferromagnetic (FM) and antiferromagnetic (AFM) transitions, respectively. The dashed line is a guide for the eye.

$PrCu_6$ has been also reported by Akashi *et al.* [3]. We estimated R_B considering that the electrical resistivity of silver paste was dominant. The boundary resistance was approximately $R_B T \simeq 10^4$ K^2/W, and the entropy change from 2.8 to 14.5 mK was on the order of gas constant R that is sufficient to account for the phase transition. We concluded that the susceptibility peak and the relaxation time maximum at T_{N2} can be ascribed to the HFE Pr nuclear magnetic phase transition at the 8c site.

Figure 4 shows the HFE nuclear magnetic ordering temperatures in Pr compounds as a function of K squared [1,2,9,31]. According to Andres [32], HF nuclear transition temperatures increase approximately in proportion to the square of K. Owing to a large enhancement factor ($1 + K_{8c} \simeq 39.4$), the nuclear transition temperature of the 8c site in $Pr_3Pd_{20}Ge_6$ is much higher than those in other Pr compounds.

We now discuss dissipation phenomena in $Pr_3Pd_{20}Ge_6$. The susceptibility (Fig. 2) shows a complicated temperature variation between 70 and 30 mK. Both χ' and χ'' show an abrupt increase at about 70 mK in zero static field; this increase is not seen at 10 mT. In static fields $\leqslant$10 mT, χ' decreases with decreasing temperature from 60 to 30 mK, and χ'' has a broad peak at $T_B = 43$ mK. The decreasing χ' below 60 mK and the peak of χ'' at T_B indicate that magnetic moments cannot follow the ac field; this indicates dissipation phenomena. We analyzed this behavior in terms of the Casimir–du Pré theory [33], which is the simplest relaxation model, described by a single relaxation time τ. The Cole-Cole plots of the ac susceptibility in the temperature range from 30 to 60 mK and in static fields of up to 10 mT are presented in Fig. 5. These plots are nearly semicircular for each static field. In our experiments, the angular frequency ω was constant, 100 rad/s (16 Hz). Therefore, the susceptibility behavior between 30 and 60 mK can be attributed to an abrupt increase in relaxation time from $\tau \ll 1/\omega$ to $\tau \gg 1/\omega$. In ultrasonic measurements of

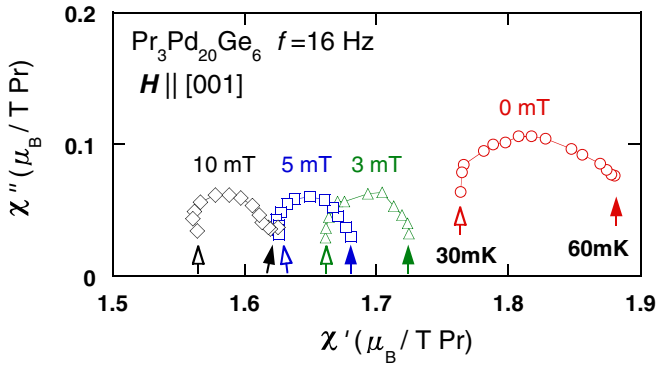

FIG. 5. (Color online) Cole-Cole plots of the ac susceptibility as a function of temperature between 30 and 60 mK in static fields of 0, 3, 5, and 10 mT along the [001] axis. The open and solid arrows indicate the susceptibilities at 30 and 60 mK, respectively.

$Pr_3Pd_{20}Ge_6$, it was reported that the attenuation coefficient of the C_{44} mode increases around 60 mK, and the elastic constant C_{44} at 20 mK shows hysteresis during a field change below 0.4 T [22]. These results support the idea that the complicated susceptibility behavior was because of dissipation phenomena caused by the Γ_5 triplet ground state at the 4a site.

One possible cause of such dissipation is the domain-wall motion ascribable to an incommensurate-to-commensurate (IC-C) transition. In the Γ_5 triplet ground states of PrB_6 and $PrPd_3$, first-order IC-C AFM transitions have been investigated by neutron scattering [34,35]. In $Pr_3Pd_{20}Si_6$, similar ac susceptibility behavior has been reported by Steinke *et al.* [13]. They have argued that a first-order IC-C AFM transition occurs at the 4a site where the magnetic ground state is a quartet (pseudospin 3/2) as a result of the formation of 4f-electron-nuclear hyperfine-coupled multiplets, as described by Aoki *et al.* [12]. Thus, it is possible that the 4a site in $Pr_3Pd_{20}Ge_6$ undergoes a first-order IC-C AFM transition at 60 mK. Further experimental and theoretical studies are necessary in order to understand details of magnetic behavior both 4f-electron and Pr nuclear magnetic moments, such as dissipation phenomenon, suppression of nuclear spin degree of freedom at the 4a site, spin structures of the 4f-electron moment and the Pr nuclear magnetic one, and the interplay between the 4a and 8c sites.

In summary, we measured the complex ac susceptibility of the clathrate compound $Pr_3Pd_{20}Ge_6$ in static fields of up to 10 mT along the [001] axis at temperatures down to 500 μK. The absence of a susceptibility anomaly at the AFQ ordering temperature $T_{Q1} = 250$ mK was confirmed. This compound showed AFM ordering of 4f-electron moments of the Γ_5 triplet ground state at the 4a site at $T_{N1} = 77$ mK. It was found that the Pr nuclear magnetic moments at the 8c site, where 4f-electron quadrupole moments of the Γ_3 doublet order at T_{Q1}, show a phase transition to an AFM state at $T_{N2} = 9$ mK. $Pr_3Pd_{20}Ge_6$ is a novel material where multiple ordering of nuclear and f-electron moments coexists on two sublattices.

This work was supported in part by Grants-in-Aid for Scientific Research from JSPS (No. 23103506 and No. 24540367) and from MEXT of Japan (No. 17002004). We acknowledge helpful discussions with H. Tsujii and experimental assistance from K. Nunomura.

[1] M. Kubota, H. R. Folle, Ch. Buchal, R. M. Mueller, and F. Pobell, Phys. Rev. Lett. **45**, 1812 (1980).
[2] Y. Karaki, M. Kubota, H. Ishimoto, and Y. Onuki, Phys. Rev. B **60**, 6246 (1999).
[3] K. Akashi, K. Kawabata, A. Matsubara, O. Ishikawa, T. Hata, H. Ishii, T. Kodama, A. Koyanagi, R. Settai, and Y. Onuki, Phys. Rev. Lett. **82**, 1297 (1999).
[4] H. Ishii, J. Low Temp. Phys. **135**, 579 (2004).
[5] P. Morin, D. Schmitt, and E. du Tremolet de Lacheisserie, J. Magn. Magn. Mater. **30**, 257 (1982).
[6] A. Yatskar, W. P. Beyermann, R. Movshovich, and P. C. Canfield, Phys. Rev. Lett. **77**, 3637 (1996).
[7] T. Morie, T. Sakakibara, H. S. Suzuki, H. Tanida, and S. Takagi, J. Phys. Soc. Jpn. **78**, 033705 (2009).
[8] A. Sakai and S. Nakatsuji, J. Phys.: Conf. Ser. **391**, 012058 (2012).
[9] S. Abe, D. Takahashi, H. Mizuno, A. Ryu, S. Asada, S. Nahaer, K. Matsumoto, H. Suzuki, and T. Kitai, Physica B: Condens. Matter **329–333**, Part 2, 637 (2003).
[10] A. Sakai, K. Kuga, and S. Nakatsuji, J. Phys. Soc. Jpn. **81**, 083702 (2012).
[11] T. U. Ito, W. Higemoto, K. Ninomiya, H. Luetkens, C. Baines, A. Sakai, and S. Nakatsuji, J. Phys. Soc. Jpn. **80**, 113703 (2011).
[12] Y. Aoki, T. Namiki, S. R. Saha, T. Tayama, T. Sakakibara, R. Shiina, H. Shiba, H. Sugawara, and H. Sato, J. Phys. Soc. Jpn. **80**, 054704 (2011).
[13] L. Steinke, K. Mitsumoto, C. F. Miclea, F. Weickert, A. Dönni, M. Akatsu, Y. Nemoto, T. Goto, H. Kitazawa, P. Thalmeier, and M. Brando, Phys. Rev. Lett. **111**, 077202 (2013).
[14] S. R. Saha, H. Sugawara, T. Namiki, Y. Aoki, and H. Sato, Phys. Rev. B **80**, 014433 (2009).
[15] T. Herrmannsdörfer, A. Dönni, P. Fischer, L. Keller, G. Böttger, M. Gutmann, H. Kitazawa, and J. Tang, J. Phys.: Condens. Matter **11**, 2929 (1999).
[16] T. Herrmannsdörfer, A. Dönni, P. Fischer, L. Keller, S. Janssen, A. Furrer, B. van den Brandt, and H. Kitazawa, Mater. Sci. Forum **443–444**, 233 (2004).
[17] Y. Koike, N. Metoki, Y. Haga, K. A. McEwen, M. Kohgi, R. Yamamoto, N. Aso, N. Tateiwa, T. Komatsubara, N. Kimura, and H. Aoki, Phys. Rev. Lett. **89**, 077202 (2002).
[18] J. Kitagawa, N. Takeda, M. Ishikawa, T. Yoshida, A. Ishiguro, N. Kimura, and T. Komatsubara, Phys. Rev. B **57**, 7450 (1998).
[19] Y. Nemoto, T. Yamaguchi, T. Horino, M. Akatsu, T. Yanagisawa, T. Goto, O. Suzuki, A. Dönni, and T. Komatsubara, Phys. Rev. B **68**, 184109 (2003).
[20] T. Goto, Y. Nemoto, T. Yamaguchi, M. Akatsu, T. Yanagisawa, O. Suzuki, and H. Kitazawa, Phys. Rev. B **70**, 184126 (2004).
[21] Y. Nemoto, T. Yanagisawa, Y. Yasumoto, H. Kobayashi, A. Yamaguchi, S. Tsuduku, T. Goto, N. Takeda, A. Ochiai, H. Sugawara, H. Sato, and H. Kitazawa, J. Phys. Soc. Jpn. **77**(Suppl. A), 153 (2008).
[22] G. Ano, M. Akatsu, K. Araki, K. Matsuo, Y. Tachikawa, K. Mitsumoto, T. Yamaguchi, Y. Nemoto, T. Goto, N. Takeda, A. Dönni, and H. Kitazawa, J. Phys. Soc. Jpn. **81**, 034710 (2012).
[23] O. Suzuki, H. Kitazawa, G. Kido, T. Yamaguchi, Y. Nemoto, and T. Goto, J. Alloys Compd. **408–412**, 107 (2006).
[24] L. Keller, A. Dönni, M. Zolliker, and T. Komatsubara, Physica B: Condens. Matter **259–261**, 336 (1999).
[25] H. Amitsuka, A. Nogami, K. Tenya, M. Yokoyama, S. Miyazaki, T. Sakakibara, M. Nakayama, N. Kimura, H. Aoki, and T. Komatsubara, J. Phys. Soc. Jpn. **71**(Suppl.), 124 (2002).
[26] J. Yoshida, S. Abe, A. Tada, H. Tsujii, K. Matsumoto, H. Suzuki, and H. S. Suzuki, J. Phys.: Conf. Ser. **150**, 042241 (2009).
[27] J. Kitagawa, N. Takeda, F. Sakai, and M. Ishikawa, J. Phys. Soc. Jpn. **68**, 3413 (1999).
[28] J. Kondo, J. Phys. Soc. Jpn. **16**, 1690 (1961).
[29] B. Bleaney, J. Appl. Phys. **34**, 1024 (1963).
[30] Y. Shimura, Y. Ohta, T. Sakakibara, A. Sakai, and S. Nakatsuji, J. Phys. Soc. Jpn. **82**, 043705 (2013).
[31] K. Andres, Cryogenics **18**, 473 (1978).
[32] K. Andres, E. Bucher, J. P. Maita, and A. S. Cooper, Phys. Rev. Lett. **28**, 1652 (1972).
[33] H. B. G. Casimir and F. K. du Pré, Physica **5**, 507 (1938).
[34] P. Burlet, J. M. Effantin, J. Rossat-Mignod, S. Kunii, and T. Kasuya, J. Phys. Colloq. **49**, C8–459 (1988).
[35] H. S. Suzuki, N. Terada, K. Kaneko, and N. Metoki (unpublished).